AUTOMATED POWER-VOLTAGE CHARACTERIZATION OF PHOTOVOLTAIC PANELS

Paul. N. MARTARI Botond S. KIREI Bogdan I. OLAIOŞ and Marina D. ŢOPA
Technical University of Cluj Napoca, Cluj Napoca, Romania
Str. Memorandumului, Nr. 28, +40264401243, botond. kirei@bel. utcluj. ro

Abstract: This paper contributes to the automated power-voltage characterization of photovoltaic panels. The proposed measurement assemblies can be used in conjunction with "quasi seek" maximum power point tracking algorithms. First, the power vs. voltage characteristics of a solar panel was traced using a common assembly that consists of the solar panel, a trimmer resistor and standard laboratory multimeters. This assembly requires a human operator to switch the trimmer resistor and the measurement intervals on the multimeters, thus not suitable for measurement automation. Next, two measurement assemblies were proposed: (i) a voltage controlled current source used to control the current drawn from the panel; (ii) a voltage controlled voltage reference used to drive the voltage on the panel. It was found in both circuits that the current sense resistor (a low side shunt resistor used for current measurement) must be varied to achieve a wide operation range with respect to the solar illumination, so a programmable resistor was added. Automatic decision over the suitable resistor value was based upon illumination measurement with a usual photoresistor. Finally the circuits were built on a test board, a virtual instrumentation was set up and the power vs. voltage characteristics of a 2W photovoltaic panel were traced.

Keywords: *maximum power point, tracking, photovoltaic cell/panel, measurement automation, voltage controlled current source, voltage controlled voltage reference, current sense resistor, low side shunt.*

I. INTRODUCTION

As the energy demand of the society rises and the conventional fossil energy carriers are becoming scarce, the need for new energy resources has risen. The response to the elevated demand seems to come from renewable energy sources, like solar, wind, hydro and bio energy. Moreover, energy efficiency is becoming the future's fifth "renewable" energy source.

The sun is the most obvious source, as it provides all the energy needed for sustaining life on earth. Actually all other renewable energy sources are derived from our sun's heat [1]. Thanks to the photovoltaic (PV) effect (the ability of some semiconductors to transform the electromagnetic radiation directly into electric current) the sunlight can be converted to electricity with the aid of solar cells. Nowadays, the efficiency of a PV cell is about 10-15% and the production cost of cells is high compared to other renewable energy sources (the production cost of solar power is expected to reach the grid parity [2] just at the end of the decade). To make the solar energy economically viable it is sought to exploit the PV cells at their maximum power through the deployment of maximum power point tracking algorithms [3]. The current literature presents a number of procedures, where the tracking is aided by a priori knowledge of power-voltage characteristics, called indirect or "quasi seek" methods, such as curve-fitting, look-up table, PV panel short-circuit and PV panel open-circuit methods [4].

The present work discusses the use of a voltage controlled current source (VCCS) and a voltage controlled voltage source (VCVS) to achieve the power-voltage characteristics (P-VC) of PV cells/panels. The proposed circuits can be used for power-voltage (P-V) characterization automation to aid "quasi seek" maximum power point tracking algorithms. In the next section the PV cell operating principle and its electric model are presented. A straightforward approach for plotting the P-VC is to measure the current and the voltage on a resistance connected in series with a PV panel. This assembly implies a human operator to switch the resistor value, thus unsuitable for measurement automation. Our proposal, presented in Section 3, is to (i) force a current or a voltage on the PV panel, (ii) use a low side shunt resistor for current measurement and (iii) trace the P-VC with a data acquisition (DAQ) system. As the solar induced current of the PV cell may vary from µA to A, a large current sensitivity range has to be guaranteed. A programmable resistor in parallel switching connection is proposed to be used as a low side shunt, thus an appropriate value can be selected from a resistor bank. The selection is based on a rough estimate of the illumination. In Section 4 the obtained results are given: first, the automated measurement assemblies are presented: a DAQ and a virtual instrument implemented on a PC. Next, several P-VC traces were achieved. Finally, conclusions are drawn in Section 5.

II. THE FOTOVOLTAIC CELL

The solar cell is an electronic device made out of two different layers of silicon doped with a small quantity of donor/acceptor atoms, thus obtaining a p-n junction (see Fig. 1) [5]. As the two layers are joined together the free electrons of the n-layer are diffused in the p-layer, the free holes in the p-layer are diffused in the n-layer. This creates an electrical field between the two layers that is a

Manuscript received April 16, 2014; revised June 6, 2014

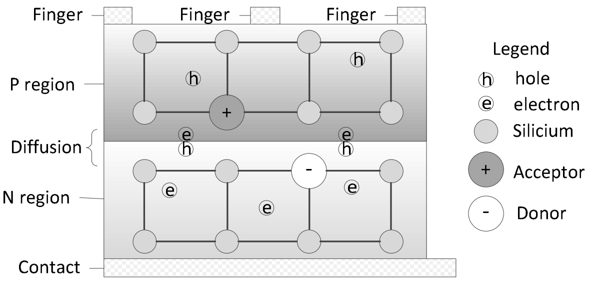

Figure 1. The photovoltaic cell model.

potential barrier to further flow. The equilibrium is reached in the junction when the electrons and holes cannot surpass the potential barrier thus they cannot move. This electrical field pulls the electrons and holes in opposite directions, thus the current can flow in only one direction: electrons can move from the p-layer to the n-layer. Metallic contacts are added to both regions to permit the current-flow. On the n-layer, which is facing the solar radiation, the contacts are made out of several metallic strips called fingers, because they must allow the light to pass to the solar cell.

The operating principle of a PV cell. When the photons of the solar radiation shine on the cell, one of the next three things can happen: (i) some photons are reflected from the top surface of the cell and from the metallic fingers, the not reflected photons penetrate in the substrate; (ii) some of them, usually the ones with less energy, pass through the cell without causing any effect; (iii) the high energy level photons create electron-hole pairs. These pairs are generated on both sides of the p-n junction. The minority charges (electrons in the p-layer and holes in the n-layer) are diffused in the junction and swept away in opposite directions (electrons to the n-layer and holes to the p-layer) by the electric field, generating a current in the cell, which is collected by the metallic strips on both sides.

Equivalent circuit of a PV cell. In the literature many lumped element models were reported, such as the one-diode model [6]. The model presented in Fig. 2 consists of (i) an ideal current generator, whose current I_L is largely determined by the solar radiation and the ambient temperature, a diode *D,* that models the p-n junction of the PV cell, the resistance R_s of the metallic contacts and a shunt resistance R_{sh} modeling electron loss in the p-n junction. In an ideal case R_s is zero and R_{sh} is infinite [7].

The PV cells current-voltage relation is expressed in the following equation:

$$I_{PV} = I_L - I_0 \cdot \left(e^{\frac{q \cdot (V_{PV} - I_{PV} \cdot R_s)}{A \cdot k \cdot T}} - 1 \right) - \frac{(V_{PV} - I_{PV} \cdot R_s)}{R_{sh}}, \quad (1)$$

where I_{PV} and V_{PV} are the current, respectively, the voltage of the solar cell, I_0 is the dark saturation current,

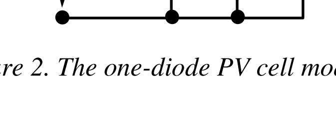

Figure 2. The one-diode PV cell model.

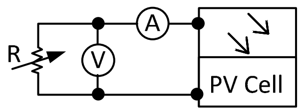

Figure 3. Assembly using a trimmer resistor.

I_L the light generated current (photocurrent), q is the charge of an electron, A is the diode quality factor, k is the Boltzmann constant, T is the absolute temperature and R_s, R_{sh} are the resistance of the metallic fingers (PV cell contacts), respectively, the shunt resistance.

The light induced current I_L is expressed as:

$$I_L = \underbrace{I_{L0} \cdot \frac{I_R}{I_{R0}}}_{irradiance} \cdot \underbrace{\left(1 + K_0 \left(T - 300\right)\right)}_{temperature}, \quad (2)$$

where I_R is the irradiance (light intensity) falling on the cell, I_{L0} is the measured solar-generated current for the irradiance I_{R0}; K_0 is a material constant of the solar cell (usually reported by the manufacturer) and T is the ambient temperature expressed in Kelvin.

The reference power-voltage characteristics. The P-VC can be plotted using an assembly presented in Fig. 3., where R symbolizes a trimmer resistor connected to the solar panel, V and A are two multimeters used for measuring the current, respectively the voltage on the PV panel. The power is the current-voltage product. The power-voltage couples are noted in a spreadsheet and finally plotted. In (2) the solar induced current I_L is influenced by the solar irradiance and the ambient temperature, thus one shall expect to obtain multiple characteristics as one of these factors changes.

The reference P-VC plots for a 2W PV panel are presented in Fig. 4. On the horizontal axes the voltage ranges from 0 to 7 V as a common practice is to cascade a number of PV cells into a panel (the current / voltage of a single cell is considered low). This PV panel is made out of 10 solar cells connected in series. On the vertical axis the measured power ranged between 0 and 2. 5 mW as all the measurements were carried out indoor (not exposed directly to the sun), in an isolated environment from ambient light, thus the solar irradiation I_R and temperature were considered constant. The resistance of a trimmer resistor was varied from a 0 Ω to 100 kΩ in 38 steps under three constant illumination conditions: 100 lx, 150 lx and 200 lx. The P - VC plots, illustrated in Fig. 4, were

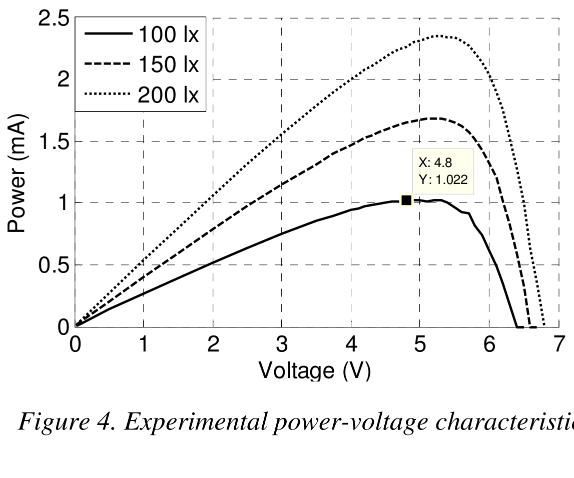

Figure 4. Experimental power-voltage characteristics

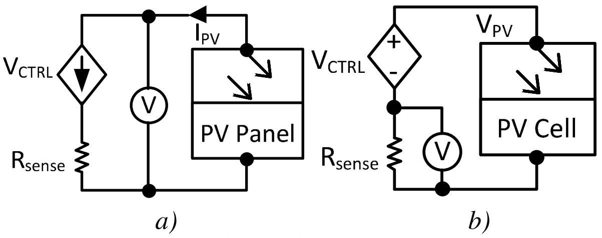

Figure 5. Power-voltage characteristics measurement with a) controlled current b) controlled voltage

obtained with standard laboratory multimeter using an intensity controlled halogen based light source and a digital lux-meter.

III. THE AUTOMATION OF POWER-VOLTAGE CHARACTERISTICS MEASUREMENT

The P-VC tracing procedure presented in the previous section requires a human operator and it is not suited for measurement automation. There are two alternative approaches to P-VC plotting, presented in Fig 5. The first one is a current controlled method (CCM) (Fig. 5a.), where the current drawn from the PV cell I_{PV} is conditioned by a controlled current source. In this configuration, the voltage on the PV cell ports is measured, while the current through the PV cell is imposed by the DAQ. The second approach is a voltage controlled method (VCM) (Fig. 5b.), where the voltage V_{PV} on the PV cell ports is conditioned by a controlled voltage reference. In this case, a current measurement is necessary (carried out with the aid of the low side shunt resistor R_{sense}), while the voltage is imposed by the DAQ.

Current controlled method. A suitable implementation for the CCM presented in Fig 6. makes use of a VCCS [9]. The opamp loop forces the output current I_{PV} to be proportional with the control voltage V_{CTRL}. The negative feedback of the opamp will adjust the current through the NMOS transistor (noted M_{PW} in Fig. 6) until the voltage on the sense resistor R_{sense} is proportional to the control voltage, V_{CTRL}. The current I_{PV} through R_{sense} can be computed with respect to the control voltage V_{CTRL}:

$$I_{PV} \cong \frac{V_{CTRL}}{R_{sense}} . \tag{3}$$

As the solar generated current I_L varies with irradiation I_R, a large change in the irradiance (2 or 3 order) can require the modification/replacement of R_{sense} to meet the operation range of the control voltage V_{CTRL}. Suppose I_L = 3 mA (a typical value of the panel when solar illumination is approximately 1000 lx). If one uses a 10 Ω resistor for R_{sense}, then he can control the VCCS with a command voltage of 0 to 3 V, drowning 0 to 3 mA. If the irradiation is decimated (I_R = 100 lx), the solar induced current is about 300 uA. With the same value of 10 Ω for R_{sense}, the control voltage can be varied from 0 to 0.3V, and this range is small with respect to the resolution of a digital to analog converter. Thus it is recommended to change R_{sense} to a 100 Ω resistor; by doing so, the control voltage range becomes 0 to 3 V. To overcome the aforementioned problem a programmable resistor in parallel switching connection is used. The programmable resistor consists of three different value resistors R_{S1}, R_{S2} and R_{S3}, being switched by transistors M_1, M_2 and M_3. The selection of the appropriate resistor is done using the control signal S_1, S_2 and S_3 provided by the DAQ. The illumination is approximated by the DAQ with the aid of a photoresistor [8] (noted LDR in Fig. 6). The photoresistor and R_3 divides the reference voltage V_{REF} into V_{LDR} that is measured by the DAQ. V_{LDR} is the input for a simple decisional algorithm that will compute the control values of S_1, S_2 and S_3. As the current is conditioned by the VCCS the voltage on the PV panel V_{PV} is measured by the DAQ. The voltage drop V_S on the sense resistor R_{sense} can be computed from the control voltage V_{CTRL}, but it is better to be measured as well.

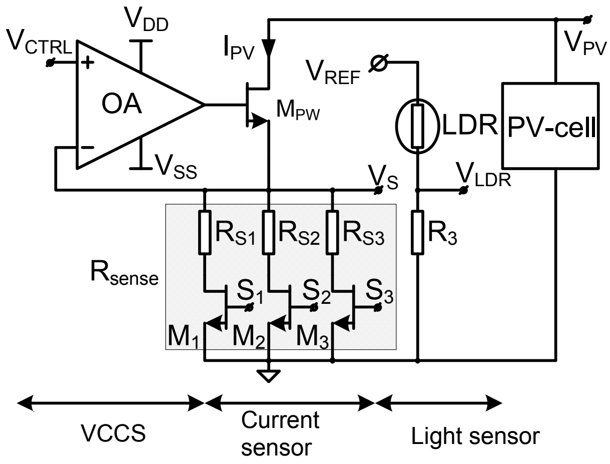

Figure 6. Current controlled measurement circuit

Voltage controlled method. The circuit used for the VCM is presented in Fig 7. Here the voltage across the PV cell is imposed by a VCVR. The VCVR has the same complexity as the VCCS and it consists of an opamp and an NMOS (noted M_{PW} in Fig. 7) enclosed in a negative feedback loop. Let us consider a small/limited control voltage V_{CTRL} range (0 to 5 V) while the open circuit voltage of the PV cell $V_{PV\text{-}OC}$ is greater then 6V.

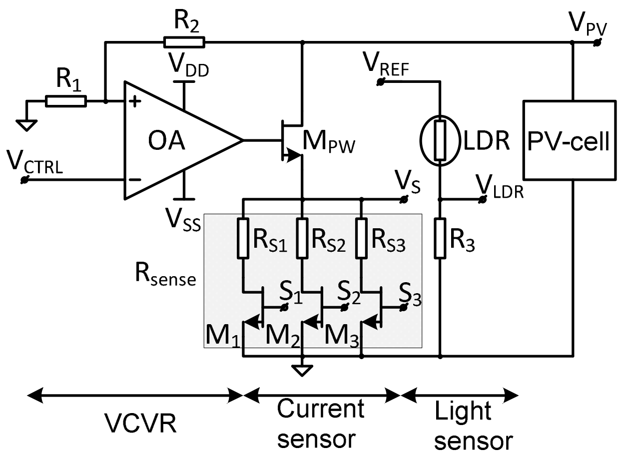

Figure 7. Voltage controlled measurement circuit

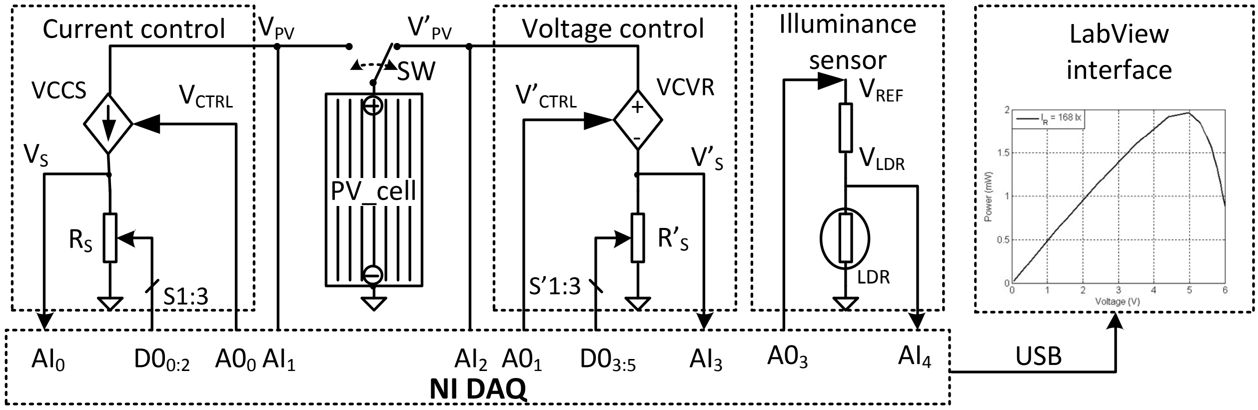

Figure 8. Proposed system for automation of power-voltage characterization for a 2W PV cell

The feedback resitors R_1 and R_2 are used for amplifying the control voltage V_{CTRL} in order to reach the V_{PV-OC}. These resitors are designed for negligable current loss in the feedback loop (R_1 and R_2 has the order of 100 kΩ). The feedback loop gain is set to 4, translating a control voltage range of 0 to 5 V into in a reference voltage range of 0 to 20 V. The current is measured using a low side shunt resistor to avoid the input common mode issues of the amplifier stage. As the shunt current is equal to the solar generated current, which may vary from a few µA to hundreds of mA, it is recommended to switch to a sense resistor appropriate for the illumination. In this circuit, the same programmable resistor is used in order to achieve the right current measurement sensitivity. The resistor selection is fully automated using an illumination intensity sensor based on a photoresistor and a simple decisional algorithm within DAQ system.

Eq. (4) describes the functionality of VCVR when the circuit is operated within a linear region.

$$V_{PV} \cong V_{CTRL} \cdot \left(1 + \frac{R_2}{R_1}\right) \tag{4}$$

Limitations of the proposed measurement methods. Considering that the VCCR and VCVR are non-ideal sources, functional limitations can be noticed. For example, the minimum voltage across the PV cell is determined by the voltage drop on the sense resistors V_S in both methods, while the maximum voltage is determined by the control voltage V_{CTRL} range, feedback loop gain and the maximum drain to source voltage V_{DS-MAX} of the power transistor M_{PW}. Except for the CCM where the maximum voltage on the PV panel ports is V_{DS-MAX}. Whenever one of the limitations is breached the VCCS and VCVS are operating in a nonlinear region because the negative feedback loop breaks. For instance, when the controlled reference voltage reaches the V_{PV-OC}, the negative feedback is lost and the remaining samples of the cell voltage and current correspond to this point. Similar for the current controlled source, when it reaches the short circuit current of the PV cell the feedback is lost and the remaining samples of the cell voltage and current correspond to this point. This aspect does not influence the measurement result mainly because the voltage and current of the PV cell are measured at the same time independently of the control loop.

IV. AUTOMATED POWER-VOLTAGE CHARACTERISTICS MEASUREMENT

Fig. 8 presents the block diagram of the proposed DAQ system for tracing the P-VC of a PV pannel. This system was used to validate the CCM and VCM presented in section III. The main blocks drawn with dotted lines in Fig. 8. are the following: a CCM assembly at the left of the figure, a VCM assembly in the middle, an illuminance sensor, the DAQ at the buttom and, at the right, the virtual instrumentation (VI) implemented on a PC in LabView.

The CCM assembly make use of a *VCCS* and a programmable sense resistor R_S. The control voltage of the *VCCS* is denoted V_{CTRL} in the figure and it is provided by the DAQ through an analog output. The resistor is programmed by the DAQ on a 3 bit wide bus, denoted $S_{1:3}$. Two voltages are measured in this case: V_{PV} and V_S, the voltage on the PV cell, respectively in the sense resistor.

The voltage controlled assembly consists of the VCVS and a current sense resistor. The DAQ controls the PV cell voltage V_{PV} through an analog output that gives the control voltage denoted V'_{CTRL}. As in the previous assembly the sense resistor R'_S is programmable by the $S'_{1:3}$ and the V'_{PV} and V'_S voltages are measured.

Both assembly are aided by a LDR based illumination sensor. The operation of the sensor is trivial: a reference voltage V_{REF} provided by the DAQ is applied on a voltage divider composed of a fix resistor and the photoresistor. As the photorsistor resistance vary with the illumination, the divided voltage V_{LDR} will be proportional with the illumination. Based on this measurement, at least a rough estimation is obtained. Furthermore the programmable resistor values are chosen to fit for three conditions: poor/medium/strong illumination.

The DAQ uses five analog inputs ($AI_{0:4}$), three analog outputs ($AO_{0:2}$) and six digital outputs ($DO_{0:5}$). As the analog inputs of the DAQ's ADC have a finite impedance it is recommended to buffer the measured signals and also scale them to fit the ADC input range.

The VI was created in the LabView environment. The operation within the virtual instrument is as follows: a linear sweep of the control voltage V_{CTRL} is applied; for each value of V_{CTRL} the parameters of interest (V_{PV} and V_S) are sampled and memorized; at the end of the voltage sweep the power is computed from the saved samples and

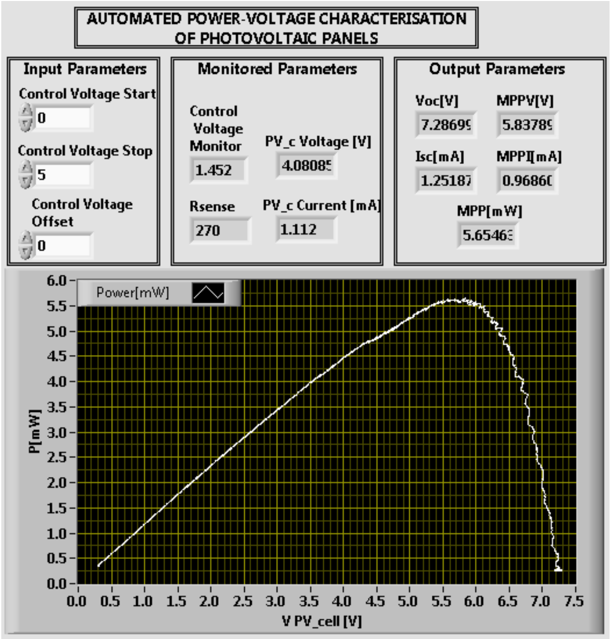

Figure 9. Front panel of the VI

the P-VC is plotted in the LabView interface (see Fig. 9). Moreover, the main parameters, such as, open circuit voltage $V_{PV\text{-}OC}$, short circuit current $I_{PV\text{-}SC}$, the maximum power point (MPP) and its coordinates are extracted in the "Output Parameters" section.

V. RESULTS

The setup. An experimental setup following the block diagram shown in Fig. 8 was built using discrete components, prototyping boards, a National Instruments USB 6009 DAQ and a PC. The setup is captured in Fig. 10. Here the main blocks are highlighted: the DAQ interface is a NI USB6009, an LDR07 photo-resistor of 17KΩ, two LM2902N quad operational amplifiers, BSN254 NMOS transistors used as switches ($M_{1:3}$) and power transistor M_{PW}, sense resistors ($R_{S1:3}$) with values of 270 Ω, 1 kΩ and 4.7 kΩ. In the bottom of the picture, only a fraction of the PV cell is shown due to its large size. The operational amplifiers are supplied with ±12 V by a standard laboratory power supply.

Calibration of the test setup. Before extracting the experimental results, a calibration procedure was carried out. The voltage and current monitors of the VI were verified and software compensated using the same standard laboratory multimeter used for reference measurements, excluding in this way the relative measurement error.

Experimental results. Using the automated system presented in section IV. several P-VC traces were obtained (see Fig. 11) under different illumination conditions. Representative examples when illumination was set to 100 lx, 150 lx and 200 lx are presented in Fig. 11 a), b), respectively c). In each trace both CCM (solid line trace) and VCM (dotted line trace) measurement results are presented.

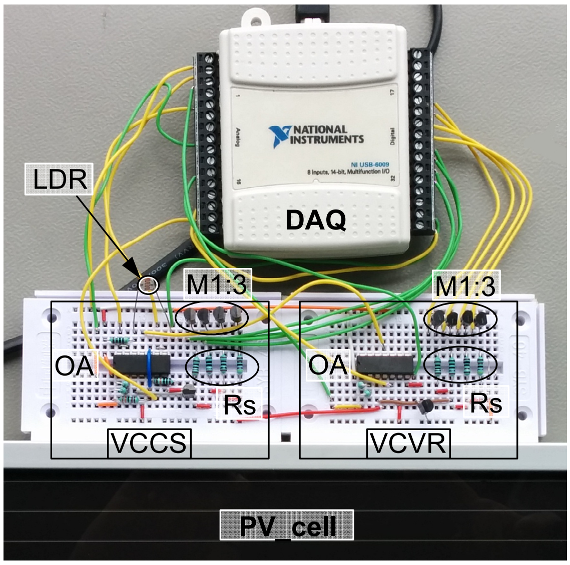

Figure 10. Test setup for P-VC trace for a 2W PV cell

a)
b)
c)

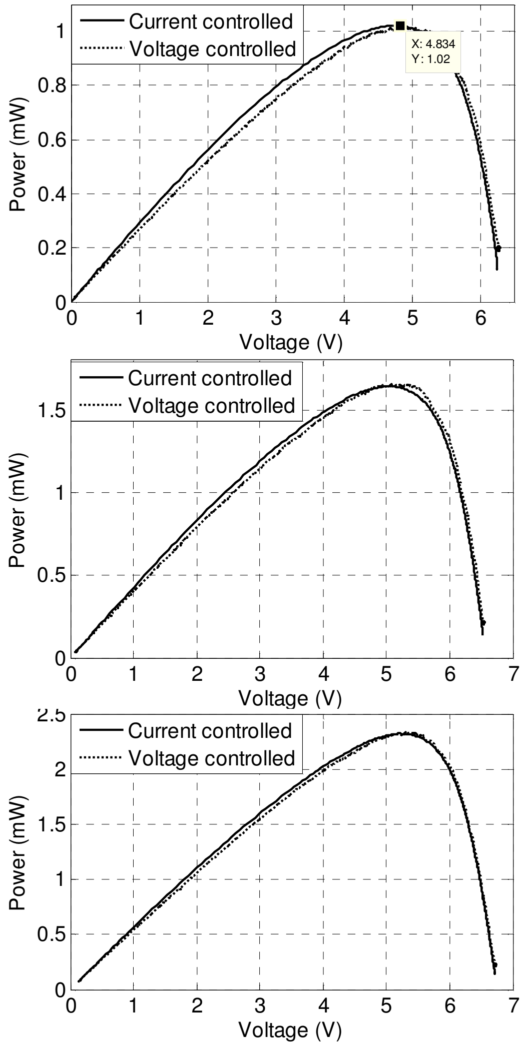

Figure 11. P-VC traces obtained with CCM and VCM under a) 100 lx b) 150 lx and c) 200 lx illumination.

Table I. The measured maximum power points

I_R	Reference	Current controlled	Voltage controlled
100 lx	1.022mW@4.8V	1.02mW@4.834V	1.02mW@4.898V
150 lx	1.685mW@5.3V	1.652mW@5.201V	1.653mW@5.301V
200 lx	2.348mW@5.3V	2.322mW@5.201V	2.333mW@5.302V

To evaluate the proposed P-VC trace methods, let us consider the measurements in Fig 4. to be a reference for the automated P-VC tracing. One can see that at 100 lx illumination the reference maximum power point is 1.022 mW at 4.8 V, while 1.02 mW was measured at 4.834 V and 4.898 V by the CCM, respectively, the VCM. The summary of the MPPs is listed in Table I.

VI. CONCLUSIONS

The power-voltage characteristics of photovoltaic panels are used by several indirect ("quasi seek") maximum power point tracking algorithms. One can trace the characteristics using a variable (trimmer) resistor connected to a solar panel and performing voltage and current measurements.

In this paper, two measurement methods are proposed to enable power vs. voltage measurement automation: a current control method is developed using a voltage controlled current source; alternatively a voltage controlled voltage reference is deployed for a voltage controlled method. These methods make use of a low side shunt resistor to sense the current flowing from the photovoltaic panel. Due to the large variation of the photovoltaic current (from a few µA to hundreds of mA) that may occur during exploitation, the proposed methods has to sense a large current interval, thus a programmable sense resistor is indicated to be used for the low side shunt. In addition, the appropriate value of the programmable resistor is selected based on illumination approximation achieved with the aid of a photoresistor.

After establishing the circuits to be used in the proposed methods an automated power vs. voltage trace assembly was implemented using discrete components connected on a breadboard, an NI USB 6009 data acquisition board and a virtual instrument developed in LabView. Automated power vs. voltage traces were achieved and compared to reference measurements, considered as a reference for the proposed methods.

Further developments are focused on adding an energy harvester circuit to supply the circuits from the solar panel. The data acquisition system may be replaced by a microcontroller fitted with memory, which can perform the measurements and save the observations. The final goal, to deploy the proposed circuit in "quasi seek" maximum power point tracking algorithms, shell be sought in the future.

ACKNOWLEDGMENTS

The authors express their gratitude for the anonymous reviewers. Their valuable observations were at great help in improving the quality and content of this paper. The first author wishes to thank Silicon Systems Transylvania Ltd. for granting him generous scholarship and substantial guidance throughout his M.Sc. and Ph.D. studies.

REFERENCES

[1]. R. B. Alley, *Earth: The Operators' Manual,* W. W. NORTON & Company, New York, 2011

[2]. K. Brankera, M. J. M. Pathaka, J. M. Pearce, "A review of solar photovoltaic levelized cost of electricity", *Renewable and Sustainable Energy Reviews*, Volume 15, Issue 9, pp. 4470-4482, 2011.

[3]. N. Onat, "Recent developments in maximum power point tracking technologies for photovoltaic systems", *International Journal of Photoenergy*, vol. 2010, Article ID 245316, 11 pages, 2010.

[4]. V. Salas, E. Olías, A. Barrado, A. Lázaro, "Review of the maximum power point tracking algorithms for stand-alone photovoltaic systems", *Solar Energy Materials and Solar Cells*, Volume 90, Issue 11, pp. 1555-1578, 2006

[5]. David Sanz Morales, *Maximum Power Point Tracking Algorithms from Photovoltaic Applications*, Thesis for the degree of Master of Science in Technology, 2010.

[6]. D. Petreuş, C. Fărcaş, I. Ciocan, "Modelling and Simulation of Photovoltaic Cells", *ACTA TECHNICA NAPOCENSIS - Electronics and Telecommunications*, Volume 49, Number 1, 2008

[7]. P. A. Lynn, *Electricity from Sunlight: An Introduction to Photovoltaics,* John Wiley & Sons, 2010

[8]. Token, "CDS Light Dependent Photoresistors – Light Dependent Photoresistors for Sensor Applications", *PGM Series datasheet*, Version 2010

[9]. R. R. Spencer, M. S. Ghausi, *Introduction to electronic circuit design*, Prentice Hall/Pearson Education, ISBN 0-201-36183-3, 2003